

MIT Open Access Articles

*Membrane-integrated superconducting
nanowire single-photon detectors*

The MIT Faculty has made this article openly available. **Please share** how this access benefits you. Your story matters.

Citation: Najafi, F., J. Mower, X. Hu, F. Bellei, P. Kharel, A. Dane, Y. Ivry, L. Cheong, K. Sunter, D. Englund and K. K. Berggren. "Membrane-integrated superconducting nanowire single-photon detectors." CLEO: QELS - Fundamental Science, San Jose, California United States, June 9-14, 2013.

As Published: http://www.opticsinfobase.org/abstract.cfm?uri=CLEO_QELS-2013-QF1A.6

Publisher: Optical Society of America

Persistent URL: <http://hdl.handle.net/1721.1/92843>

Version: Author's final manuscript: final author's manuscript post peer review, without publisher's formatting or copy editing

Terms of use: Creative Commons Attribution-Noncommercial-Share Alike



Membrane-integrated superconducting nanowire single-photon detectors

F. Najafi*, J. Mower, X. Hu, F. Bellei, P. Kharel, A. Dane, Y. Ivry, L. Cheong, K. Sunter, D. Englund and K. K. Berggren

Department of Electrical Engineering and Computer Science, Massachusetts Institute of Technology, 77 Massachusetts Avenue, Cambridge, Massachusetts 02139, United States

*f_najafi@mit.edu

Abstract: We integrated superconducting nanowire single-photon detectors on sub-400-nm-thick silicon nitride membranes, which can then be transferred and aligned to photonic structures on a secondary chip with sub-micron placement accuracy.

OCIS codes: (040.5570) Quantum detectors; (040.3060) Infrared; (040.3780) Low light level, (250.0250) Optoelectronics

Superconducting nanowire single-photon detectors (SNSPDs) [1] based on sub-100-nm-wide niobium nitride (NbN) nanowires offer an unmatched combination of sensitivity [2], speed [3] and timing jitter [4] in the near-infrared range. To date, approaches to integrate SNSPDs with photonic structures [5-7] were only compatible with a handful of substrate materials and required additional fabrication steps on the sample. These steps can be incompatible with complex photonic integrated circuits (PICs). Based on a micron-scale flip-chip concept [8], we have developed a technology that enables integration of SNSPDs on PICs without exposing the PIC to chemicals or high temperatures. We used this method to integrate SNSPDs with silicon waveguides designed for 1550 nm center wavelength.

The scanning electron micrograph (SEM) of a waveguide-SNSPD consisting of 95-nm-wide nanowires arranged in a 200-nm-pitch meander pattern is shown in Fig. 1. The nanowires were fabricated by patterning a NbN film grown on top of a SiN_x-on-Si substrate. The thickness of the SiN_x layer was 350 nm. The NbN layer, grown using reactive magnetron sputtering of Nb in Ar/N₂ plasma at 800 °C substrate temperature, had a sheet resistance of ~ 500 Ω/square and a critical temperature of 10.5 K. The size of the detector (marked in yellow in Fig. 1(a)) was constrained by the accuracy of membrane placement ($\pm 0.5 \mu\text{m}$), the width of the waveguide ($\sim 0.5 \mu\text{m}$) and the minimum meander length (min. L_M) required to reach > 90 % optical absorption in the detector when placed on a waveguide. The results of the COMSOL simulation [9] used to calculate L_M are shown in Fig. 1(d).

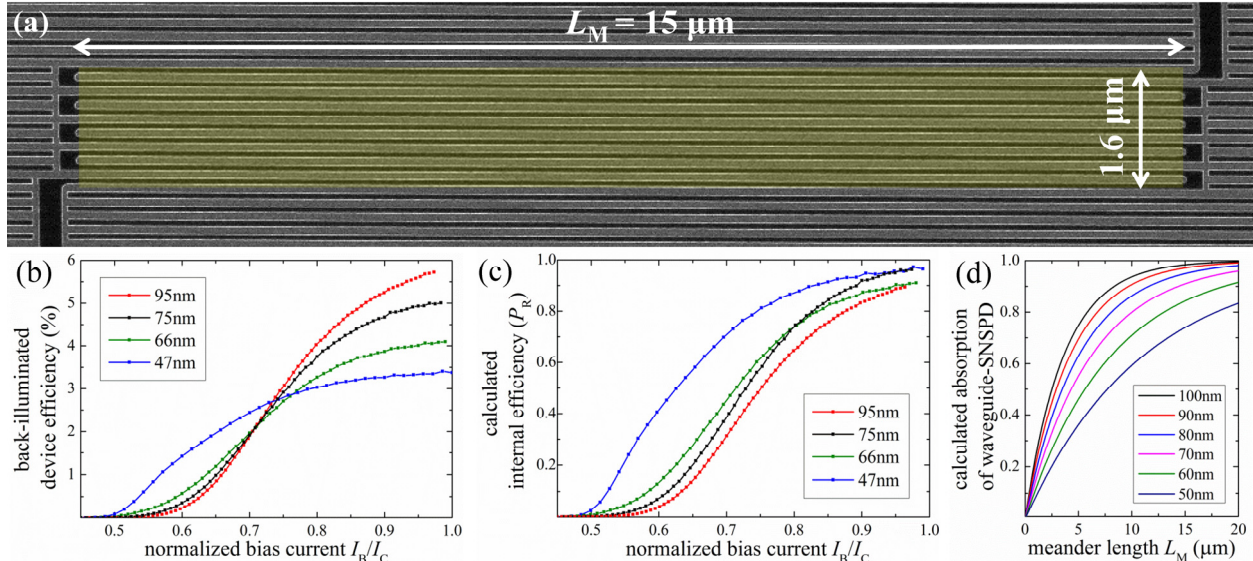


Fig. 1. (a) SEM of waveguide-SNSPD HSQ mask (95-nm-wide nanowires) on top of NbN. The pitch was 200 nm and the length of the meander structure L_M was 15 μm , resulting in a waveguide-to-nanowire coupling length of 45 μm when the detector is placed on top of a 500-nm-wide waveguide. (b) Back-illuminated device detection efficiency (DE) vs bias current (I_B) normalized by critical current (I_C). The experimental error is $\pm 5\%$ of the DE value. The DE is plotted for nanowire widths 47 nm ($I_C = 7 \mu\text{A}$), 66 nm ($I_C = 10.1 \mu\text{A}$), 75nm ($I_C = 12.2 \mu\text{A}$) and 95 nm ($I_C = 14.9 \mu\text{A}$). (c) Calculated internal efficiency (P_R) of the same detectors as in (b). (d) Calculated optical absorption vs meander length of an SNSPD (200 nm meander pitch) on top of a 500-nm-wide silicon waveguide. The COMSOL simulations used equations outlined in Ref. [9]. Furthermore it was assumed that the waveguide and the SNSPD were separated by a 20-nm-thick HSQ layer (residual resist from previous lithography steps).

The detectors were characterized at 2.4 K using a fiber-coupled incoherent polarized light source with 1540 nm center wavelength. The back-illuminated device detection efficiency (DE) vs bias current (I_B) is shown in Fig. 1(b). Since these devices were designed for evanescent side-coupling to a waveguide [9, 5] rather than back-coupling, the on-chip detection efficiency [6] of the waveguide-SNSPD is mainly limited by the ‘internal efficiency’, P_R [10], which is the probability that the SNSPD produces an output signal once it has absorbed the photon. We estimated P_R by dividing the measured DE by the calculated optical absorption for back-illumination. The results are shown in Figure 1(c). While narrower nanowires reach $P_R > 90\%$ at lower bias currents and show approximately constant (‘saturated’) DE close to the critical current (I_C), they inhibit a lower electrical output pulse amplitude (which is proportional to I_B). A lower signal amplitude, i.e. a smaller signal-to-noise ratio, results in higher timing jitter. For waveguide-integration, detectors with $I_C > 13\ \mu\text{A}$ were used to ensure sub-35-ps timing jitter (Fig. 2(c)).

After cryogenic characterization, detectors that reached saturation were chosen for the subsequent membrane fabrication process: the surface of the chip was cleared of Au and NbN except for a small area around the SNSPD. Trenches were defined around the detector area via photolithography. The photomask was used to etch trenches through the SiN_x layer down to the silicon substrate via CF_4 reactive ion etching. The underlying silicon was then removed via isotropic dry etch in XeF_2 , resulting in SNSPDs on suspended SiN_x membranes. The membrane-SNSPD is shown in Fig. 2(a). Micro-manipulated tungsten probes (300 nm tip diameter) were used to break the four micro-bridges, pick up the membrane and visually align the membrane-SNSPD to the waveguide and to prefabricated gold pads on the waveguide chip that matched the gold pads on the membrane.

The resulting waveguide-integrated SNSPD is shown in Fig. 2(b). We are currently working on efficient fiber coupling to the waveguides in order to characterize the (system) detection efficiency of this waveguide-SNSPD system. Preliminary cryogenic measurements on back-illuminated membrane-SNSPDs that were transferred on a secondary substrate showed that (1) the adhesion between membranes and secondary substrate was resistant to thermal cycling; (2) the membrane fabrication and transfer process resulted in a tolerable shift of the detector properties (reduction of I_C by less than 15 %); and (3) the physical and electrical contact between the membrane and the secondary substrate were sufficient to cool the detector in a continuous-flow cryostat, where we measured sub-35-ps timing jitter. While the photonic structures demonstrated here are waveguides, this technology could be applied to other PICs that require on-chip integration and near-field single-photon detection.

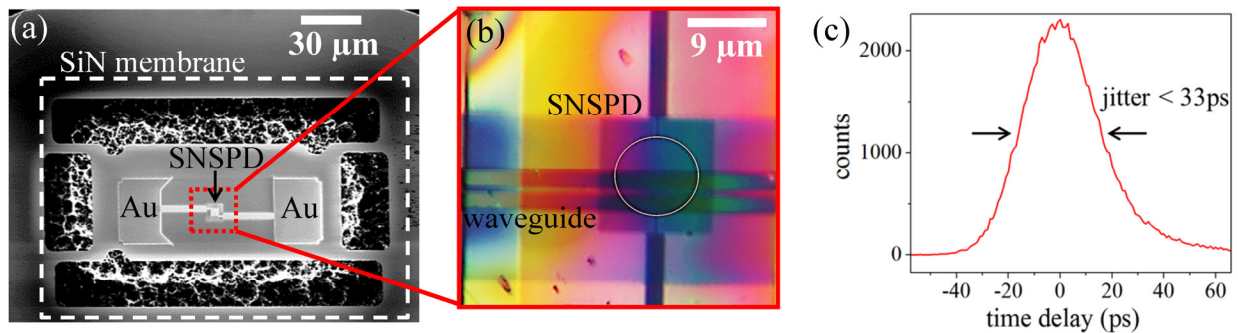


Fig. 2. (a) SEM of a SiN_x membrane ($\sim 350\ \text{nm}$ thick) with SNSPD on top. (b) Optical micrograph of a membrane-SNSPD that was transferred and aligned to a Si waveguide on a PIC chip. (c) Instrument Response Function (IRF) of a membrane-SNSPD transferred onto a secondary substrate. The IRF was measured using a mode-locked fiber-coupled laser with sub-ps-pulse-width and 1550 nm wavelength. We measured sub-35-ps timing jitter for detectors with $I_C > 13\ \mu\text{A}$.

- [1] G. Gol'tsman et al., Applied Physics Letters 79, 705-707 (2001);
- [2] A. Korneev et al., IEEE Transactions on Applied Superconductivity 15, 571-574 (2005);
- [3] R. Hadfield, Nature Photonics 3, 696-705;
- [4] E. Dauler et al., IEEE Transactions on Applied Superconductivity 17, 1051-8223 (2007);
- [5] J. Sprengers et al., Applied Physics Letters 99, 181110 (2011);
- [6] W. Pernice et al., Nature Communications 3: 1325 (2012);
- [7] K. Rosfjord et al., Optics Express 14, 527-34 (2006);
- [8] D. Englund et al., U.S. Patent Application No. 13/633,647;
- [9] X. Hu et al., IEEE Transactions on Applied Superconductivity 19, 336-340 (2009);
- [10] A. Semenov et al., The European Physical Journal B 47, 495-501 (2005).